

Article

## Flow Linear Dichroism to Probe Binding of Aromatic Molecules and DNA to Single-Walled Carbon Nanotubes

Jascindra Rajendra, Mark Baxendale, Laurence Georges Dit Rap, and Alison Rodger

*J. Am. Chem. Soc.*, **2004**, 126 (36), 11182-11188 • DOI: 10.1021/ja048720j • Publication Date (Web): 20 August 2004

Downloaded from <http://pubs.acs.org> on April 1, 2009

### More About This Article

Additional resources and features associated with this article are available within the HTML version:

- Supporting Information
- Links to the 1 articles that cite this article, as of the time of this article download
- Access to high resolution figures
- Links to articles and content related to this article
- Copyright permission to reproduce figures and/or text from this article

[View the Full Text HTML](#)



## Flow Linear Dichroism to Probe Binding of Aromatic Molecules and DNA to Single-Walled Carbon Nanotubes

Jascindra Rajendra,<sup>†</sup> Mark Baxendale,<sup>‡</sup> Laurence Georges Dit Rap,<sup>†</sup> and Alison Rodger<sup>\*†</sup>

Contribution from the Department of Chemistry, University of Warwick, Coventry, CV4 7AL, U.K., and Department of Physics, Molecular and Materials Physics Group, Queen Mary, University of London, Mile End Road, London E1 4NS, U.K.

Received March 5, 2004; E-mail: a.rodger@warwick.ac.uk

**Abstract:** Structures of carbon nanotube/ligand complexes were studied by flow linear dichroism (the differential absorption of light polarized parallel and perpendicular to the flow orientation direction) with the aim of establishing linear dichroism as a technique to study such systems. Anthracene, naphthalene, and DNA were chosen as ligands, and the potential for flow linear dichroism to probe ligands noncovalently (as well as covalently) bound to single-walled nanotubes is reported. Linear dichroism enables the determination of approximate orientations of the ligands on the carbon nanotubes.

### 1. Introduction

Carbon nanotubes (CNTs), as a new allotrope of carbon with extraordinary properties and many captivating potential applications, have attracted much interest since they were discovered in 1991 by Iijima.<sup>1</sup> Carbon nanotubes are fascinating structures for fundamental science and technological applications in the new field of nanoscience.<sup>2</sup> Due to their unusual geometry and their structural and electronic properties, these carbon nanostructures are viewed as promising building blocks for molecular electronics and as reinforcing fillers in composite materials. A lot of research targeting applications of multiwalled (MW) and single-walled (SW) CNTs (SWNTs) has been undertaken, including their utilization as field emitters, electrodes of lithium-ion batteries, tips for scanning probe microscopes (SPM), nanoelectronic devices, and supports in catalysis.<sup>3</sup> Recently, significant progress has been made in both the chemical functionalization and manipulation of CNTs.<sup>4</sup> In this work we have been focusing on the noncovalent functionalization of CNTs.

Since the discovery of carbon nanotubes, thousands of papers have been published on MW and SW CNTs but the field is in desperate need of new structural characterization techniques for CNT systems. Previous work has quantified the structural anisotropy that develops in surfactant-stabilized aqueous nanotube suspensions under steady shear flow by the combination of small-angle polarized light scattering and optical microscopy in situ.<sup>5,6</sup> Chemisorptive attachment of anthracene and several

derivatives onto the sidewalls of SWNTs has been investigated using FT-IR, fluorescence, and absorbance spectroscopies, and some discussion of the changes in spectra of SWNT–anthracene absorptive adducts compared to free anthracene and its derivatives has been given.<sup>7</sup> Absorbance data probing the effect of anthracene adsorption on SWNTs has been determined between 300 and 400 nm, where anthracene has pronounced vibronic structure in its electronic absorbance spectrum. In a related application, the physisorption of aromatic molecules on the graphite basal plane has been investigated by NMR experiments, neutron diffraction, and Penning ionization electron spectroscopy.<sup>8,9</sup> However, structural information about physisorbed films of naphthalene and anthracene molecules on graphite is still lacking, and these approaches have yet to be extended to CNTs. In this paper we report the first use of flow linear dichroism with SWNTs and SWNT–ligand adducts and show it has potential for probing ligands noncovalently (as well as covalently) bound to the SWNT. With the use of UV–vis flow linear dichroism on an adapted Jasco J-715 circular dichroism spectropolarimeter we are able to probe the interaction over a wide wavelength range (190–800 nm) and thus use polarized spectroscopy to give more information about the nature of the ligand–CNT interactions.

Interpretation of the flow LD data ideally requires the transition moments of the species being studied to be known. In the case of nanotubes, there is very little information about their spectroscopy in the near and far UV regions, which are

\* Corresponding author. Phone: +44-24-76523234. Fax: +44-24-76524112.

<sup>†</sup> University of Warwick.

<sup>‡</sup> University of London.

(1) Liang, Q.; Gao, L. Z.; Li, Q.; Tang, S. H.; Liu, B. C.; Yu, Z. L. *Carbon* **2001**, *39*, 897–903.

(2) Bernier, P.; Maser, W.; Jouret, C.; Loiseau, A.; de la Chapelle, M. L.; Lefrant, S.; Lee, R.; Fischer, J. E. *Carbon* **1998**, *36*, 675–680.

(3) Saito, T.; Matsushige, K.; Tanaka, K. *Physica B: Condens. Matter* **2002**, *323*, 280–283.

(4) Azamian, B. R.; Davis, J. J.; Coleman, K. S.; Bagshaw, C. B.; Green, M. L. H. *J. Am. Chem. Soc.* **2002**, *124*, 12664–12665.

(5) Hobbie, E. K.; Wang, H.; Kim, H.; Han, C. C.; Grulke, E. A.; Obrzut, J. *Rev. Sci. Instrum.* **2003**, *74*, 1244–1250.

(6) Hobbie, E. K.; Wang, H.; Kim, H.; Lin-Gibson, S.; Grulke, E. A. *Phys. Fluids* **2003**, *15*, 1196–1202.

(7) Zhang, J.; Lee, J. K.; Wu, Y.; Murray, R. W. *Nano Lett.* **2003**, *3*, 403–407.

(8) Tabony, J.; White, J. W.; Delachaume, J. C.; Coulon, M. *Surf. Sci. Lett.* **1980**, *95*, L282–L288.

(9) Bondi, C.; Baglioni, P.; Taddei, G. *Chem. Phys.* **1985**, *96*, 277–285.

the regions of particular interest for the ligands we have chosen to study. A few papers have been published on transition moment polarizations of fullerenes determined using induced circular dichroism<sup>10</sup> or on optical measurements with polarized light.<sup>11</sup> In the case of CNTs, it generally seems to be assumed that there is no UV spectroscopy and the focus has been on near infrared, infrared, and Raman work. In fact, as discussed below, the CNTs do have UV absorbance; it is just very unstructured and often masked by light scattering.

In addition to aromatic molecules, e.g., naphthalene and anthracene, as nanotube ligands, we were interested in probing the binding of DNA to CNTs. There are reports in the literature of strong interactions between DNA and carbon nanotubes;<sup>12</sup> however, the nature of such interactions is not yet clear. Techniques used to study DNA/nanotube systems have included UV and IR absorbance spectroscopy<sup>13,14</sup> and surface-enhanced infrared absorption (SEIRA)<sup>15</sup> as well as transmission electron microscopy (TEM). None of these techniques give information on how the DNA molecules interact with CNTs, and in most cases the CNT/DNA system has been deposited on a solid surface. A recent report of DNA solubilizing nanotubes uses AFM and absorbance spectroscopy to prove this is in fact the case; however, there was no attempt to characterize the interaction.<sup>16</sup> One motivation for studying the interaction of CNTs with DNA is the potential use of CNTs as atomic force microscopy tips to probe biomacromolecules.<sup>17</sup> In this context or independently, any means of immobilizing DNA onto solid supports may provide a means of using DNA as a recognition agent, e.g., for complementary DNA or for specific proteins.

## 2. Materials and Methods

**Materials.** SWNTs were obtained from Dynamic Enterprises Ltd. These had been synthesized by the catalytic arc discharge method.<sup>18</sup> To overcome problems due to inhomogeneity of the samples, stock solutions of SWNT (0.5 mg/mL) were prepared. The stock solution of SWNTs was obtained by sonicating the SWNTs for 2 min in aqueous sodium dodecyl sulfate (SDS, Sigma, 9 mM) at a concentration slightly above the CMC (which is 8.5 mM) of SDS to give a viscous solution of concentration 0.5 mg of SWNT per milliliter of SDS.<sup>19</sup> The analytes were then added to the SWNT SDS solutions as outlined below.

A number of different SWNTs purification methods were attempted. All purified SWNT samples used to collect data reported in this paper were purified by refluxing in 3 M nitric acid at 120 °C for 13.5 h and then washed with water (18.2 MΩ). Purity was investigated by transmission electron microscopy (TEM).<sup>4</sup>

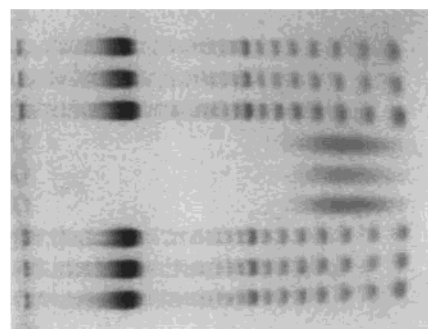


**Figure 1.** Gel electrophoresis analysis of a DNA sample after sonicating for about 2–3 h using 100 base pair ladder (where bands in the top and bottom three lanes are from right to left 100, 200, 300, 400, 500 bp, etc.). The middle three lanes contained the sonicated DNA sample to be used in the fragmented DNA–carbon nanotube experiments. The sonicated DNA sizes range from 200 to 400 base pairs.

All solvents (BDH laboratories) were analytical grade except for hexane, which was spectroscopic grade. Calf thymus DNA (ct-DNA), naphthalene, and anthracene were obtained from Sigma Aldrich Chemical Co. and used as received. A stock solution of ct-DNA (0.4 mg/mL) was prepared in SDS (9 mM).

All spectroscopy experiments except those noted as being in hexane were performed with aqueous SDS (9 mM) as the solvent. For the spectroscopy experiments, in the first instance a potential SWNT ligand was added to a SWNT suspension ( $\sim 0.1$  mg mL<sup>-1</sup>) in SDS to a concentration of  $\sim 0.5$  mg mL<sup>-1</sup> for the small molecules and 0.1 mg mL<sup>-1</sup> for the DNA, though in some cases further dilution (with SDS (9 mM)) was required to avoid excessive absorbance. Anthracene was introduced to the single-walled suspension either by adding the solid and vortexing the sample to facilitate its solubilization or by adding a concentrated methanolic solution to the SWNT suspension. Other polyaromatic hydrocarbons were introduced from methanolic solutions. Short DNAs of  $\sim 200$ –400 base pairs (as determined by gel electrophoresis, Figure 1) were obtained by sonicating an aqueous SDS solutions of ct-DNA for about 2–3 h,<sup>20</sup> and aliquots were added to the SWNT suspension. All preparations were left overnight to equilibrate before spectroscopic measurements were performed. The DNA/SWNT samples gave the same results if the spectra were measured immediately upon mixing; however, leaving the samples for days resulted in some precipitation from solution and unsatisfactory spectroscopy. For the same reason the SWNT stock solution was always prepared fresh as SWNTs are not stable in SDS for more than 1 week because they aggregate together and fall out of solution. SDS (9 mM) was used as the baseline for all spectra; however, for the LD it was found that the sample without rotation could be used as the baseline because it overlaid on the rotating SDS spectrum. In fact, this coincidence of the baselines was a good check on system performance.

**Spectroscopy.** Absorbance: UV–visible absorbance spectra were recorded using a Cary 1E spectrophotometer.

**Linear dichroism (LD):** LD is the difference in anisotropic absorption of light polarized in planes parallel ( $A_{\parallel}$ ) and perpendicular ( $A_{\perp}$ ) to the direction of orientation.<sup>21</sup>

$$LD = A_{\parallel} - A_{\perp} \quad (1)$$

An isotropic collection of molecules will have no LD, while a group of molecules whose transition moments are macroscopically oriented will absorb differing amounts of parallel and perpendicular plane-polarized light, producing a nonzero LD spectrum. For a perfectly

- (10) Marconi, G.; Mayer, B.; Klein, C. T.; Kohler, G. *Chem. Phys. Lett.* **1996**, *260*, 589–594.
- (11) Bommeli, F.; Degiorgi, L.; Wachter, P.; Bacsá, W. S.; deHeer, W. A.; Forro, L. *Solid State Commun.* **1996**, *99*, 513–517.
- (12) Tsang, S. C.; Guo, Z. J.; Chen, Y. K.; Green, M. L. H.; Hill, H. A. O.; Hambley, T. W.; Sadler, P. J. *Angew. Chem., Int. Ed. Engl.* **1997**, *36*, 2198–2200.
- (13) Buzaneva, E.; Karlash, A.; Yakovkin, K.; Shtogun, Y.; Putselyk, S.; Zherebetskiy, D.; Gorchinskiy, A.; Popova, G.; Prilutska, S.; Matyshevska, O.; Prilutskyy, Y.; Lytvyn, P.; Scharff, P.; Eklund, P. *Mater. Sci. Eng., C: Biomimetic Supramol. Syst.* **2002**, *19*, 41–45.
- (14) Matyshevska, O. P.; Karlash, A. Y.; Shtogun, Y. V.; Benilov, A.; Kirgizov, Y.; Gorchinskiy, K. O.; Buzaneva, E. V.; Prilutskyy, Y. I.; Scharff, P. *Mater. Sci. Eng., C: Biomimetic Supramol. Syst.* **2001**, *15*, 249–252.
- (15) Dovbeshko, G. I.; Repnytska, O. P.; Obraztsova, E. D.; Shtogun, Y. V. *Chem. Phys. Lett.* **2003**, *372*, 432–437.
- (16) Nakashima, N.; Okuzono, S.; Murakami, H.; Nakai, T.; Yoshikawa, K. *Chem. Lett.* **2003**, *32*, 456–457.
- (17) Guo, Z. J.; Sadler, P. J.; Tsang, S. C. *Adv. Mater.* **1998**, *10*, 701–703.
- (18) Journet, C.; Maser, W. K.; Bernier, P.; Loiseau, A.; delaChapelle, M. L.; Lefrant, S.; Deniard, P.; Lee, R.; Fischer, J. E. *Nature* **1997**, *388*, 756–758.

- (19) Doorn, S. K.; Fields, R. E.; Hu, H.; Hamon, M. A.; Haddon, R. C.; Selegue, J. P.; Majidi, V. *J. Am. Chem. Soc.* **2002**, *124*, 3169–3174.
- (20) Elsner, H. I.; Lindblad, E. B. *DNA–J. Mol. Cell. Biol.* **1989**, *8*, 697–701.
- (21) Rodger, A.; Nordén, B. *Circular Dichroism and Linear Dichroism*; Oxford University Press: New York, 1997.

oriented molecule the measured LD would equal  $A_{\parallel}$  ( $>0$ ) for a transition polarized exactly parallel to the orientation direction or  $-A_{\perp}$  ( $<0$ ) for a transition polarized exactly perpendicular to a uniaxial orientation direction. Thus, qualitative information about the orientation of molecules in space can be extracted from the sign of the LD. A more quantitative picture of molecular alignment can be obtained from the reduced LD ( $LD^r$ )<sup>21</sup>

$$LD^r = \frac{LD}{A} = \frac{3}{2}S(3 \cos^2 \alpha - 1) \quad (2)$$

where  $A$  is the normal isotropic absorption and constitutes an average over all possible orientations,  $\alpha$  is the angle between the transition moment of interest and the macroscopic orientation axis, and  $S$  is the orientation parameter (1 for perfect orientation and 0 for an isotropic solution).

Flow LD spectra were recorded using a Jasco J-715 circular dichroism spectropolarimeter with extended sample compartment adapted for LD measurements. The Couette cell used to flow orient the samples in most of the experiments has a  $\text{CaF}_2$  rotating central cylinder and  $\text{CaF}_2$  windows in an outer stationary sleeve separated by a gap of  $50 \mu\text{m}$ , making a path length of  $100 \mu\text{m}$ .<sup>22</sup> The photomultiplier tube was moved into the sample compartment next to the LD cell using a housing fabricated for the instrument by European Chirality Services<sup>23</sup> to reduce artifacts due to scattered light. Some experiments were performed with a small volume quartz LD cell whose outer quartz cylinder has an internal diameter of  $\sim 3 \text{ mm}$  and rotates while the inner cylinder is a stationary  $\sim 2.5 \text{ mm}$  diameter quartz rod.<sup>24</sup> The latter cell had the advantages of having focusing optics after the sample to collect scattered light and a demountable sample holding component which facilitates cleaning. The PMT was left in the standard position with this cell. The rotation speed used in the experiments was  $\sim 1000 \text{ rpm}$ .

**Gel Electrophoresis.** A stock solution of Tris borate buffer (0.45 M) was prepared by dissolving Tris(hydroxymethyl)-aminomethane (27 g, 0.1 M, Amersham Pharmacia Biotech) and orthoboric acid (13.75 g, 0.1 M, BDH) in distilled water (500 mL). The pH of the buffer was adjusted to pH 7 with concentrated hydrochloric acid. On the day of the experiment a Tris borate buffer working solution (0.045 M) was prepared by diluting Tris borate buffer stock solution (50 mL, 0.45 M) to 500 mL with distilled water.

A 2% w/v agarose gel was prepared by heating agarose (0.67 g, Amersham Pharmacia Biotech) in Tris borate buffer working solution (33.5 mL, 0.045 M) to  $95 \text{ }^\circ\text{C}$  with constant stirring until all agarose had dissolved. The solution was allowed to cool to  $60 \text{ }^\circ\text{C}$  and then cast onto a gel tray ( $110 \times 100 \text{ mm}$ ) with an 11-tooth comb used to produce sample wells already in position (depth of gel  $\approx 4 \text{ mm}$ ). The gel was allowed to dry for 1 h at room temperature. The gel tray was then positioned in a Pharmacia GNA-100 submarine tank and just submerged under Tris borate buffer working solution. The comb was removed, and  $6 \mu\text{L}$  of each sample was loaded into the individual wells.

A Pharmacia Electrophoresis power supply ECPS 3000/150 was used. The power supply was initially set to  $\sim 70 \text{ V}$  and turned off when the markers had moved  $3/4$  of the way up the gel. The gel tray was removed from the tank and placed in a glass dish containing ethidium

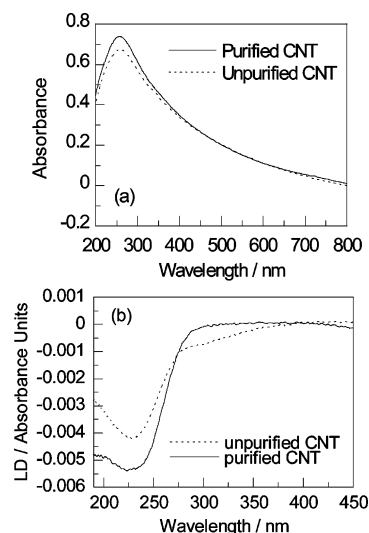


**Figure 2.** (a) Absorbance spectrum and (b) flow LD spectrum of unpurified (dashed line) and purified (solid line) carbon nanotubes (0.1 mg/mL) dissolved in 9 mM SDS. All spectra have had baselines of SDS (9 mM) without SWNTs subtracted.

bromide ( $40 \mu\text{L}$  of  $10 \text{ mg/mL}$ , Amersham Pharmacia Biotech in  $100 \text{ mL}$  of Tris borate buffer working solution). The gel was stained for 15 min and then visualized under a UV lamp (at  $254 \text{ nm}$ ) and photographed using a UVP White/UV transilluminator. Photographic images were obtained using Grab-it 2.0 software (Synoptics Ltd).

**Transmission Electron Microscopy (TEM).** A carbon-coated copper mesh screen,  $2\text{--}3 \text{ nm}$  in diameter, was used to hold the samples for TEM.<sup>25</sup> A drop of the sample was spread over the carbon-coated copper grid in a thin film of material less than  $100 \text{ nm}$  thick. The grids were placed on filter paper to remove the excess material and dried at room temperature for 1 day, and then the image was captured. TEM images were obtained using a JEOL 2000FX transmission electron micrograph with a beam accelerating voltage of  $200 \text{ kV}$ .

### 3. Results and Discussion

The lack of information about the UV spectroscopy of CNTs in the literature probably correlates with the fact that the spectroscopy observed there is quite broad and in most spectrometers would be dominated by the scattering of light by the CNTs.<sup>26</sup> In our case we have either moved the photomultiplier tube very close to the LD cell or used a small volume LD cell with focusing lenses before and after the sample to ensure that most of the unabsorbed light is detected rather than scattered in our LD experiments.

**Linear Dichroism (LD) of Nanotubes.** The aim of this work was to determine if LD could be used to probe the structures of nanotube/ligand complexes. LD is measured on systems that are either intrinsically oriented or oriented during the experiment. Figure 2 shows LD spectra of unpurified and purified SWNTs, from which it is evident that the carbon nanotubes can be oriented by Couette flow. The signal is not due simply to light scattering or turbidity dichroism (i.e., loss of photons rather than absorbance), which would result in a positive LD signal as well as a positive absorbance with a (wavelength)<sup>-n</sup> dependence.<sup>27</sup>

(25) Sawyer, L. C.; Grubb, D. *Polymer microscopy*, 2nd ed.; Chapman and Hall: New York, 1995; pp 17–33.

(26) Kataura, H.; Kumazawa, Y.; Maniwa, Y.; Umez, I.; Suzuki, S.; Ohtsuka, Y.; Achiba, Y. *Synth. Met.* **1999**, *103*, 2555–2558.

(27) Mikati, N.; Nordh, J.; Nordén, B. *J. Phys. Chem.* **1987**, *91*, 6048–6055.

(22) Rodger, A.; Rajendra, J.; Marrington, R.; Ardhammar, M.; Nordén, B.; Hirst, J. D.; Gilbert, A. T. B.; Dafforn, T. R.; Halsall, D. J.; Woolhead, C. A.; Robinson, C.; Pinheiro, T. J. T.; Kazlauskaitė, J.; Seymour, M.; Perez, N.; Hannon, M. J. *Phys. Chem. Chem. Phys.* **2002**, *4*, 4051–4057.

(23) Rodger, A.; Rajendra, J.; Marrington, R.; Mortimer, R.; Andrews, T.; Hirst, J. B.; Gilbert, A. T. B.; Marrington, R.; Halsall, D.; Dafforn, T.; Ardhammar, M.; Nordén, B.; Woolhead, C. A.; Robinson, C.; Pinheiro, T.; Kazlauskaitė J.; Seymour, M.; Perez, N.; Hannon, M. J. Flow oriented linear dichroism to probe protein orientation in membrane environments. In *Biophysical Chemistry: Membranes and Proteins*; Templar, R. H., Leatherbarrow, R., Eds.; Royal Society of Chemistry: Cambridge, 2002; pp 3–19.

(24) Marrington, R.; Dafforn, T. R.; Halsall, D. J.; Mortimer, R.; Andrews, T.; Rodger, A. Micro Volume Couette Flow Sample Orientation for Absorbance and Fluorescence Linear Dichroism. *Biophys. J.* **2004**.

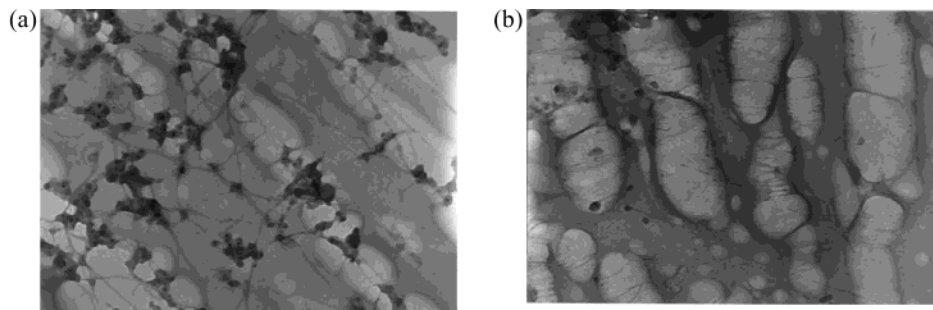


**Figure 3.** Transmission electron microscopy (TEM) images at  $\times 25k$  magnification of (a) SWNTs and (b) SWNTs purified by refluxing in 3 M hydrochloric acid at 120 °C for 13.5 h.

In this case, we observe both a maximum in the absorbance spectrum and a negative maximum in the LD spectra at  $\sim 225$  nm. It is interesting to note that the purified sample has no LD signal above 275 nm, whereas the unpurified sample does. In addition, the signal for a given mass/volume concentration is larger for the purified sample below 275 nm. Thus, the purification process removes the impurities that absorb above 270 nm. Since the surfaces of single-walled nanotubes produced by catalytic arc discharge are normally coated with amorphous carbon or fullerene materials in which the metal catalyst remains embedded,<sup>28</sup> the differences between the unpurified and purified spectra suggest that the long wavelength signal is due to these materials and that the lower wavelength signal is intrinsic to the CNT. In support of this conclusion, TEM images (Figure 3) show that most of the surface material has indeed been removed by the purification process. The 225 nm region spectrum is presumably due to in-plane polarized  $\pi-\pi^*$  transitions. That the LD is negative requires the polarization of this transition to be less than  $54^\circ$  from the average nanotube axis. Whether different geometries of SWNTs would have different LD signs at 225 nm or the expected long-axis polarization is at shorter wavelength are questions that cannot yet be answered. However, with improved nanotube production techniques the former question could be answered. Determination of the LD sign below 200 nm will require a further reduction in the light scattering contribution to the LD. This work is in progress.

**Nanotubes and Small Aromatic Molecules.** Given that the SWNT were oriented in the Couette flow, we were interested in seeing whether LD could be used to probe the interaction of small aromatic molecules with the nanotubes. A chromophore specifically bound to an oriented nanotube will also be oriented and is expected to show an LD signal under its own absorption bands. Our preliminary experiments showed signals for most of the molecules investigated; however, the signals were small, so we chose to focus on anthracene and naphthalene which have very distinctive spectroscopic signatures. These molecules are thus good tests for proof of principle and method development.

**Anthracene.** The LD spectrum of Figure 4c shows that anthracene binds to the SWNTs since anthracene has no intrinsic LD signal of its own in SDS solution. The 380 nm region of the anthracene spectrum is intrinsically polarized along the short axis of the anthracene molecule, though it has a long-axis component 'borrowed' from the 250 nm band. Polyethylene film LD of anthracene shows it to be dominated by the short-axis component.<sup>21</sup> That it has a negative signal tells us that the short

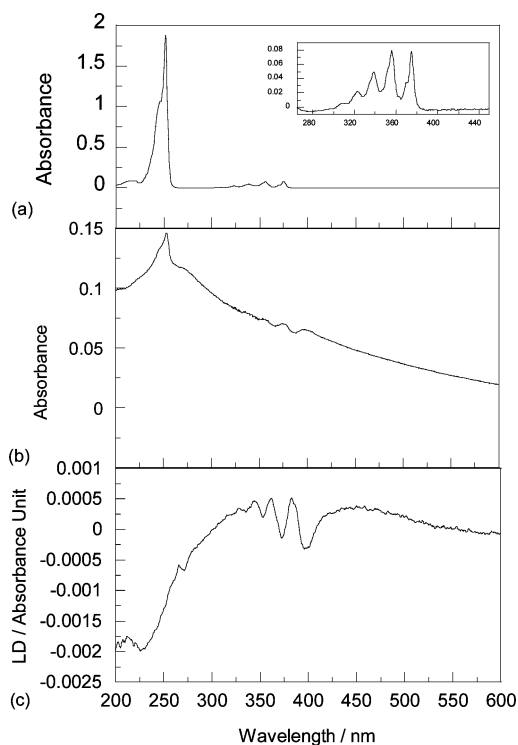


**Figure 4.** (a) Absorption spectrum of anthracene (0.0125 mg/mL, 1 mm path length) dissolved in hexane. The spectrum from 265 to 450 nm is enlarged in the insert. (b) Absorption (in 1 mm path length) and (c) LD spectrum of SWNT/anthracene complex. SWNT (0.025 mg/mL) in aqueous SDS (9 mM) by sonication was added to concentrated anthracene (0.25 mg) in methanol; baselines of, respectively, the absorbance and LD of SDS (9 mM) were subtracted in each case.

axis of anthracene is oriented at an angle larger than  $54^\circ$  with respect to the long axis of the SWNT. The shift to significantly longer wavelength than that of anthracene in hexane suggests a significant degree of  $\pi-\pi$  interactions between the anthracene and the SWNT or between anthracene molecules. The 250 nm region of the anthracene spectrum (a long-axis-polarized transition) is difficult to probe in the presence of SWNT due in part to the broad CNT absorbance (see above) in this region. The LD has a small indication of a positive band in the region of 265 nm and perhaps a negative signal at  $\sim 275$  nm overlaid on top of the broad CNT LD (Figure 4c). This is significantly red shifted compared with the hexane wavelength of 250 nm and corresponds to a small broad shoulder in the CNT plus anthracene absorbance (Figure 4b). The 250 nm sharp band in the absorbance (Figure 4b) correlates with a free anthracene concentration of  $\sim 0.002$  mg/mL (total anthracene concentration is 0.0125 mg/mL). The most puzzling aspect of this spectrum

(28) Zhang, Y.; Shi, Z.; Gu, Z.; Iijima, S. *Carbon* **2000**, *38*, 2055–2059.

is that the 380 nm LD band has a significantly larger signal than the 265 nm band despite the absorbance intensity of this band being  $\sim 20$  times smaller in the hexane absorbance spectrum (Figure 4a). However, absorbance of anthracene in the presence of the SWNTs shows the same effect, suggesting that some electronic interaction is taking place between the anthracene and SWNT.

The most obvious binding mode of the anthracene to the CNT is lying flat on the surface. If an anthracene molecule is indeed oriented flat on the surface of a nanotube oriented parallel to the long axis of the nanotube, then the 265 nm region transition has  $\alpha = 0$  and the 380 nm band has  $\alpha = 90^\circ$  (from eq 2), giving, respectively, positive and negative signals (as observed), but the 380 nm region should be 1/40 the magnitude of the 260 nm region.

An alternative explanation is that the anthracene is oriented with the short axis perpendicular to the surface of the SWNT and there is no preferred orientation on the nanotube. The symmetry of the situation is then analogous to that of a ligand binding to a flow-deformed liposome and we may write<sup>22,29</sup>

$$LD^r = \frac{3S}{4}(1 - 3\cos^2\beta) \quad (3)$$

where  $\beta$  is the angle the transition moment of interest makes with the normal to the nanotube surface. Transition moments perpendicular to the surface (380 nm region short-axis polarized here) thus have  $LD^r/3S = -1/2$ . If the average angle of the long-axis moment lies at an angle close to  $54^\circ$  from the CNT long axis, then we would predict LD signals of similar magnitude to those observed. However, the broadening and apparent loss of magnitude of the 250 nm absorbance signal is still not accounted for.

To investigate the role of packing effects on the observed LD spectra, three different concentrations 0.01, 0.02, and 0.05 mg/mL, corresponding to 10%, 20%, and 50% of full coverage, respectively (if all anthracene molecules are in solution—which is unlikely to be the case—and lie flat on the surface of the nanotube), of anthracene were chosen to analyze the effect of loading on the SWNTs (at concentration 0.1 mg/mL in SDS (9 mM)). It was not possible to measure accurate data at lower loadings, and the SWNT concentration could not be increased. The 250 nm anthracene absorbance is essentially lost, indicating little or no free anthracene in these preparations.

**Naphthalene.** The absorbance and LD spectra of naphthalene and SWNTs are shown in Figure 6 at reasonably high naphthalene concentrations. The LD spectrum of Figure 6c shows that naphthalene binds to the SWNTs since it has no intrinsic LD signal of its own in SDS solution. The naphthalene absorbance loses its structure upon interaction with the SWNT and shifts to longer wavelengths. The longer wavelength short-axis-polarized band LD, in contrast to the situation with anthracene, has an LD signal smaller than the long-axis polarized 220 nm region, consistent with its smaller absorbance magnitude. After subtracting the nanotube LD signal from the naphthalene/SWNTs signal (Figure 6d), there is a positive/negative couplet with a sharp negative LD signal at 218 nm and a broad longer wavelength positive signal. The LD baseline

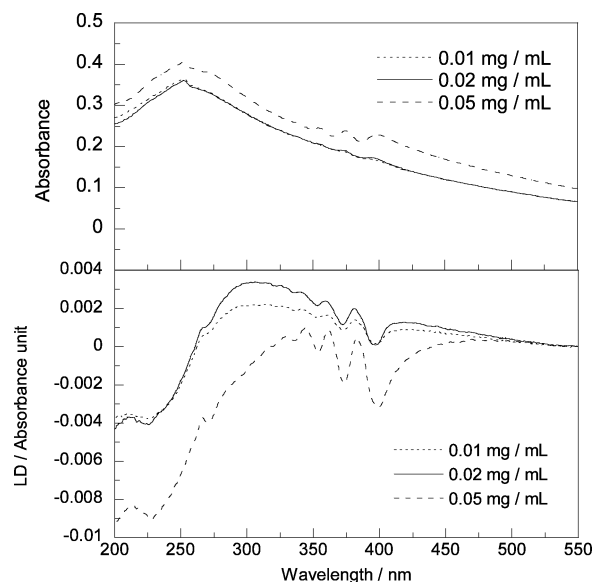


**Figure 5.** (a) Absorption and (b) linear dichroism spectra of different concentrations of anthracene with SWNTs (0.1 mg/mL)/SDS (9 mM). Anthracene was added to the SWNT solution as a concentrated methanolic solution, making final concentrations of 0.01, 0.02, and 0.05 mg/mL anthracene solutions. Baselines of, respectively, the absorbance and LD of SDS (9 mM) were subtracted in each case.

of Figure 6d is flat as we would normally expect after subtracting the intrinsic SWNT contribution. This is in contrast to the situation with anthracene, which argues for some kind of absorbance intensity transfer from the anthracene 250 nm band to the SWNT.

To probe the effect of surface coverage of the SWNT by naphthalene, data were collected for different concentrations of naphthalene (Figure 7). We assumed that the naphthalene absorbance coefficient is unchanged by its physisorption and used this extinction coefficient to calculate the amount of naphthalene in solution. The ratio of absorbance of naphthalene (Figure 6a) in a solution of known concentration to that seen in the difference spectrum of Figure 7b then gives the concentration of adsorbed naphthalene in a solution of SWNT/naphthalene complex.<sup>7</sup> The coverage of the following concentrations of naphthalene 0.2, 0.4, and 0.6 mg/mL were then calculated as 1.4%, 15%, and 26%, respectively, assuming the naphthalene lies flat on the surface of the SWNT (any absorbance suppression will mean these numbers are an underestimate). Though the signal-to-noise ratio is significantly worse at the lower loadings, from Figure 7d it is clear that the spectral shape depends significantly on the coverage with the 220 nm couplet not being evident at the lowest loading. Intriguingly, the long wavelength band is comparatively more intense at the lower loadings, as in the case of the anthracene spectrum (whose lower solubility precludes higher concentrations being studied). This leads one to speculate that the loss of the higher energy absorbance and LD intensity at lower loadings in both cases is due to some coupling between the nanotube and naphthalene or anthracene chromophore. This effect is stronger for anthracene, where a flat baseline could not be obtained by subtracting the absorbance of free SWNT.

At the lower loadings, both naphthalene bands have positive LD signals. A simple polyethylene stretched film LD experiment shows that both bands are dominantly long-axis polarized (data not shown). (Even though the electronic origin of the first band

(29) Ardhammar, M.; Lincoln, P.; Nordén, B. *J. Phys. Chem. B* **2001**, *105*, 11363–11368.

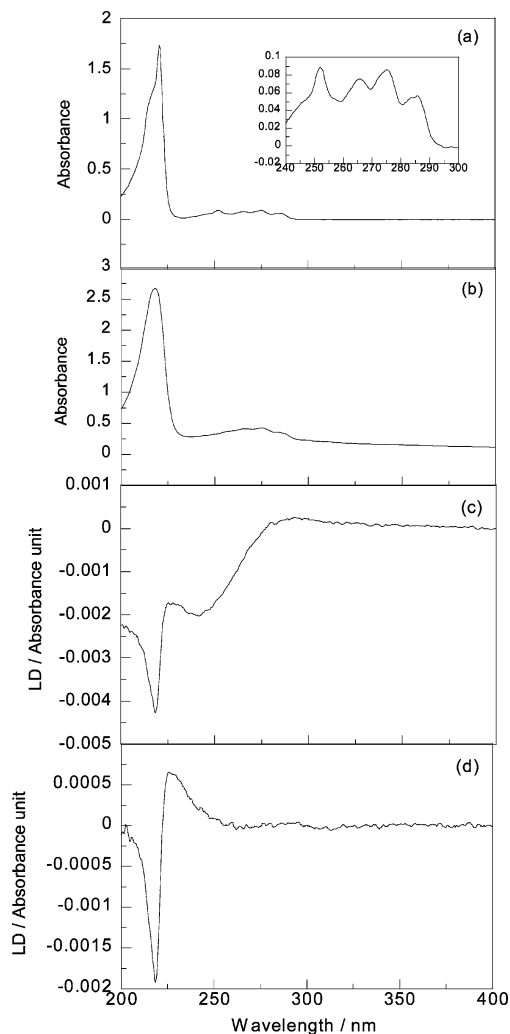


**Figure 6.** (a) Absorption spectrum of naphthalene (0.017 mg/mL) dissolved in hexane with 1 mm path length. The spectrum from 240 to 300 nm is enlarged in the insert. (b) Absorption and (c) LD spectra of SWNT/naphthalene complex. Naphthalene was added to the SWNT solution (0.1 mg/mL in 9 mM SDS) as a concentrated methanolic solution, making a final concentration of 0.5 mg/mL naphthalene solution. Baselines of, respectively, the absorbance and LD of SDS (9 mM) were subtracted in each case. (d) LD signal of naphthalene after subtracting the LD signal of SWNTs from SWNT/naphthalene signal

is short-axis polarized, the intensity is dominated by vibronic borrowing from the allowed shorter wavelength band). Thus, the naphthalene long axis is oriented at an angle smaller than  $54^\circ$  from the SWNT long axis than perpendicular to it. The data are consistent with the naphthalene lying flat on the surface but with no other orientation preference. The decrease in the positive signal of the longer wavelength band and the appearance of a sharp negative signal at 218 nm as the loading is increased is consistent with the naphthalene gradually adopting a mode with the long axis perpendicular to the SWNT long axis, i.e., poking out from the SWNT, and loss of coupling of these transitions to the electronic structure of the SWNT. The excitonic nature of this band is consistent with the degenerate coupling between transitions of  $\pi$ -stacked naphthalene units.

**Nanotubes and DNA.** Scanning tunneling microscopy (STM), transmission electron microscopy (TEM), and atomic force microscopy (AFM) are the main methods currently used for the visualization of DNA.<sup>17</sup> TEM images have been used to show that DNA binds to carbon nanotubes; still the nature of

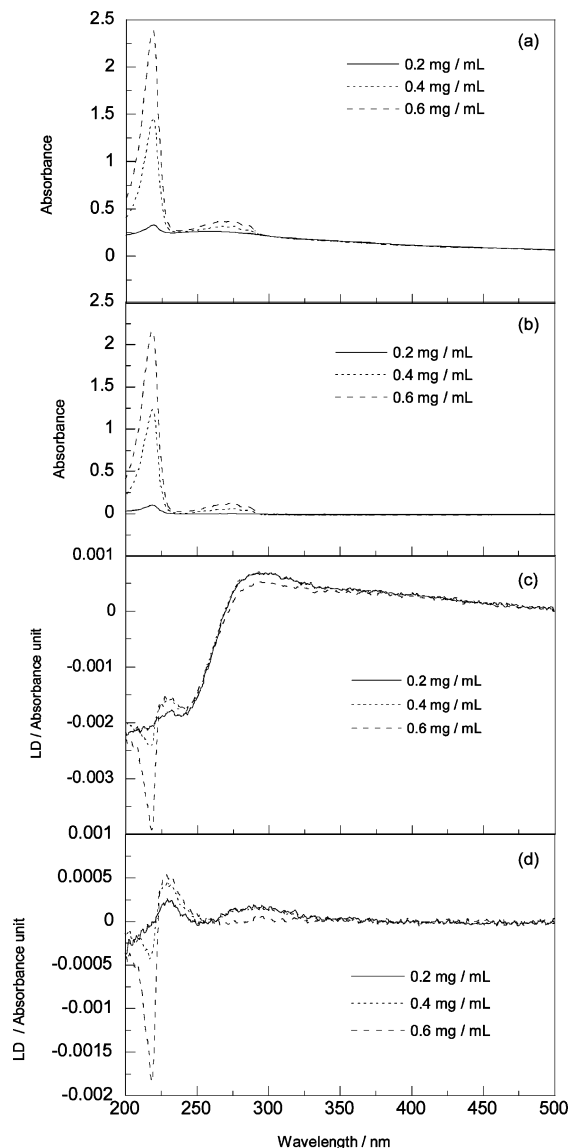


**Figure 7.** (a) Absorption spectra of different concentrations of naphthalene in SWNTs (0.1 mg/mL)/SDS (9 mM) solution. SWNTs/naphthalene complexes were prepared by adding different amounts (0.2, 0.4, and 0.6 mg) of methanol dissolved naphthalene to 1 mL of SWNTs (0.1 mg/mL) in SDS (9 mM) solution to make final concentrations of 0.2, 0.4, and 0.6 mg/mL naphthalene solutions. (b) Difference absorption spectra of part (a) spectra obtained by subtracting the absorbance spectrum of SWNT (0.1 mg/mL) from the absorbance spectra of 0.2, 0.4, and 0.6 mg/mL naphthalene/SWNTs complexes. (c) LD spectra of different concentrations of naphthalene in SWNTs (0.1 mg/mL)/SDS (9 mM) solution. SWNTs/naphthalene complexes were prepared by adding different amounts (0.2, 0.4, and 0.6 mg) of methanol-dissolved naphthalene to 1 mL of SWNTs (0.1 mg/mL) in SDS (9 mM) solution and making final naphthalene concentrations of 0.2, 0.4, and 0.6 mg/mL. (d) Difference LD spectrum of 0.2, 0.4, and 0.6 mg/mL naphthalene obtained by subtracting the LD spectrum of SWNT (0.1 mg/mL) from the LD spectra of 0.2, 0.4, and 0.6 mg/mL naphthalene/SWNTs complexes.

such interaction is not clear.<sup>17</sup> We were interested in investigating the ability of LD to probe the interaction of DNA and nanotubes in aqueous solution. Figure 8a shows that the sonicated DNA samples were not long enough to show significant orientation in our experiments. As shown in Figure 8d, it is clear that the DNA is binding to carbon nanotubes because the DNA-associated carbon nanotube gives a larger LD signal than the sum of the LD spectrum of DNA and the SWNT in isolation. Thus, the DNA is binding to the SWNTs and is

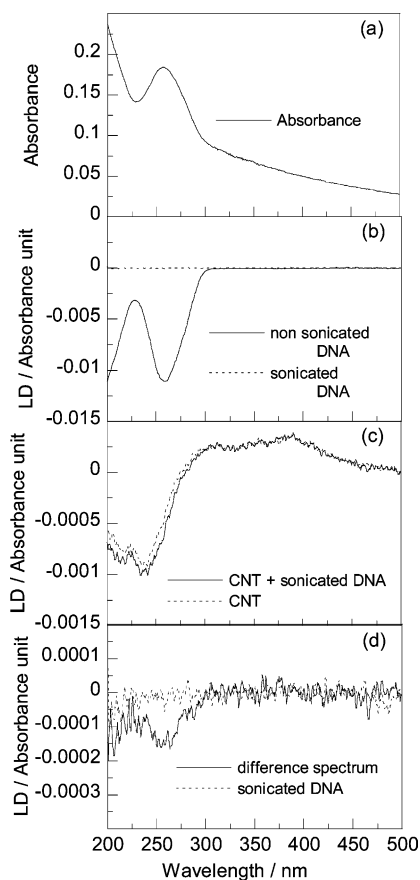


**Figure 8.** (a) Absorbance spectrum of sonicated DNA (0.033 mg/mL)/SWNTs (0.033 mg/mL) complex in SDS (9 mM) solution. The nonsonicated DNA absorbance overlays the sonicated absorbance at the same concentration. (b) LD spectrum of unsonicated (solid line) and sonicated (dashed lines) ct-DNA in aqueous SDS (9 mM). (c) LD spectra of SWNT (0.033 mg/mL)/sonicated DNA (0.033 mg/mL) (solid line) and LD spectrum of SWNT (0.033 mg/mL) (dashed line). (d) Difference LD spectrum of SWNT (0.033 mg/mL)/sonicated DNA (0.033 mg/mL) complex and SWNT (0.033 mg/mL) spectrum compared with sonicated DNA (0.033 mg/mL, dashed line) spectrum. All spectra had SDS (9 mM) baselines subtracted.

being flow oriented when the SWNTs are oriented. The small size of the signal suggests very little is binding (not entirely surprising given the anionic SDS required to solubilize the CNTs) and/or the DNA is wrapped about the nanotube at an oblique angle, thus having the bases oriented fairly close to the magic angle of  $54.7^\circ$ .

Visual confirmation that the DNA was indeed binding to the SWNTs was obtained using TEM (Figure 9), which also suggests that DNA molecules tend to cover the surface of the nanotubes evenly. Platinated and iodated DNA oligomers and

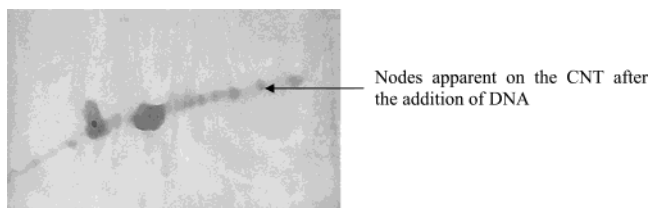


**Figure 9.** TEM images at  $\times 40k$  magnification of DNA associated carbon nanotubes.

their immobilization on CNT have been visualized under high-resolution TEM;<sup>12</sup> however, we were unable to improve the resolution of our unsubstituted DNA. Nodes (indicated by an arrow) are apparent on the CNT, showing that DNA is binding to CNTs (no nodes are apparent for CNT images in the absence of DNA, Figure 3). In this image we could also see the amorphous carbon attached to the carbon nanotubes.

#### 4. Conclusion

Three ligands, anthracene, naphthalene, and sonicated calf thymus DNA, were chosen to establish the potential of flow linear dichroism to probe ligands binding to single-walled carbon nanotubes. In each case clear evidence of binding was observed.

However, the data raise questions about the nature of the SWNT/ligand interactions especially in the case of the aromatic molecules where the spectroscopy of the ligands is significantly perturbed by their interaction with the nanotubes. The spectra for naphthalene are consistent with it adopting a mode where it lies flat on the surface at low loading, quite possible with no orientation preference or else aligned with the SWNT long axis, and at higher loadings it appears to begin adopting a mode with its long axis perpendicular to the surface. The anthracene experiments were more limited in concentration range, and our current proposal is that the anthracene is observed in a mode with its short axis perpendicular to the SWNT surface. The anthracene long-axis-polarized transition interacts significantly with the SWNT. In the case of naphthalene, when it lies flat on the surface of the SWNT the long-axis-polarized transitions are broadened and reduced in intensity. When naphthalene is oriented perpendicular to the surface, its long-axis-polarized transition is less perturbed.

A significant advantage of the LD, in addition to potentially providing orientation information, is that molecules free in solution are invisible so we only probe those bound to the CNTs.

**Acknowledgment.** Steve York's help with the electron microscopy is gratefully acknowledged.

JA048720J